Supporting Information

Synthesis, crystal structure, DNA interaction and *in vitro* anticancer activity of a Cu(II) complex of purpurin: Dual poison for human DNA topoisomerase I and II

Piyal Das[a], Chetan Kumar Jain[b,d], Sanjoy K. Dey[c], Rajat Saha[c], Abhishek Dutta Chowdhury[a], Susanta Roychoudhury[b], Sanjay Kumar[c], Hemanta Kumar Majumder[d] Saurabh Das*[a]

Supplementary contents

Preparation of solutions

LH_3 of ~96% purity was purchased from Sigma-Aldrich and purified by re-crystallization from ethanol-water mixtures. The compound being photosensitive was stored in the dark. Solution of LH_3 was prepared in ethanol (1 mM) just before use. Aqueous Tris buffer was used to maintain pH. Sodium nitrate (AR) and sodium chloride (AR) was used for maintaining ionic strength for studies in solution. Triple distilled water was used in all experiments. Calf thymus DNA, purchased from Sigma-Aldrich was dissolved in triple distilled water. Concentration of DNA solution (in terms of nucleotide) was determined from the absorbance at 260 nm taking molar extinction coefficient as 6,600 M^{-1} cm^{-1}. Absorbance at 280 nm was also recorded and the ratio A_{260}/A_{280} was calculated. The ratio being $1.8<A_{260}/A_{280}>1.9$, indicated the DNA that was used was sufficiently free of protein. Quality of CT DNA was also verified from the CD spectra at 260 nm using a CD spectropolarimeter, J815, JASCO [1]. Proton dissociation of LH_3 (50 μM) in the presence of 25 μM aqueous $Cu(NO_3)_2$was determined with the help of a pH-metric titration [2,3].

Determination of stoichiometry of the Cu(II) complex of LH_3 at different pH

Stoichiometry was determined by mole-ratio method keeping either concentration of Cu(II) or LH_3 constant and varying the other component. Change in absorbance was measured at 513 nm and plotted against ratio of LH_3 to Cu(II) [Fig. S1(a)] or Cu(II) to LH_3 [Fig. S1(b)]. Straight lines were obtained intersection of which determines stoichiometry of the complex. Fig. S1(a) & S1(b) suggest formation of a 1:2 metal-ligand complex at neutral pH. However, in more alkaline conditions, pH > 8.54 [Fig. S1(c)], both 1:1 and 1:2 complexes were formed [2].

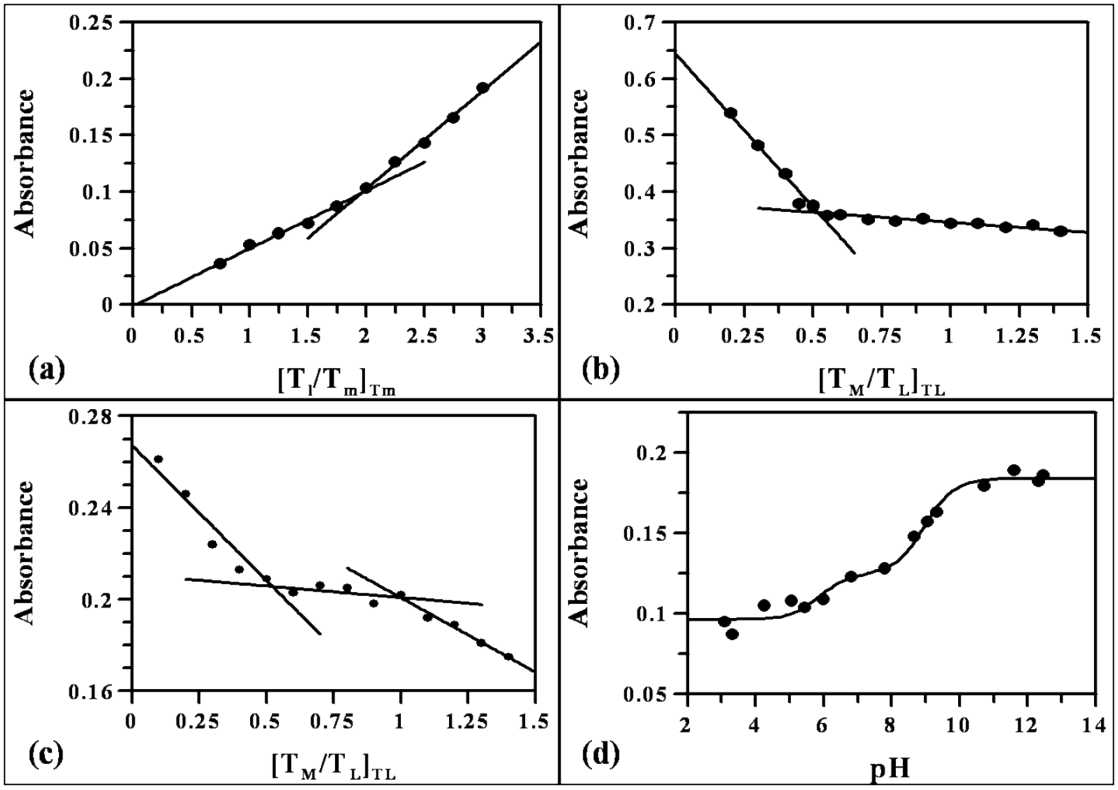

Figure S1. (a) and (b): Mole-ratio plot showing the interaction of $Cu^{(II)}$ with LH_3 in solution at neutral pH; (c): Mole-ratio plot showing the interaction of $Cu^{(II)}$ with LH_3 in solution at pH 8.54. (d) Spectrophotometric titration of LH_3 in presence of Cu(II) in the ratio 2:1, shown by the variation of absorbance at 513 nm; [$NaNO_3$] = 10 mM, T = 298 K.

Determination of stability constant of $Cu^{(II)}$-$(LH_2)_2$ in solution:

Formation constant for the complex was determined with the help of a spectrophotometric titration where Cu(II) and LH_3 were taken in the ratio 1:2. The change in absorbance at 513 nm over the pH range 2.5 to 11.0 showed a gradual increase with a corresponding increase in pH that became constant beyond pH 10. In the pH range 4.5 to 7, a proton from the –OH group at C_1 got ionized (Eq. 1) [3].

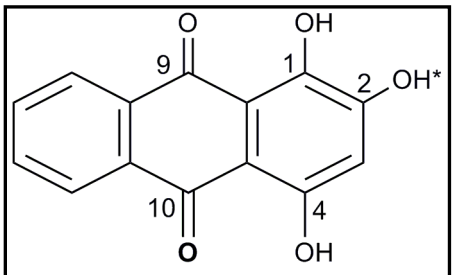

Purpurin or LH_3 or LH_2H^*

$$L\ H^*H_2 \rightleftharpoons LH^*H^- + H^+ \qquad (1)$$

The deprotonated LH_3 reacted with Cu(II) resulting in equilibrium 2.

$$Cu^{2+} + 2LH_3 \rightleftharpoons Cu(LH_2)_2 + 2H^+ \qquad (2)$$

The change in absorbance (A_{obs}) at 513 nm could be described as:

$$A_{obs} = A_1/(1 + 10^{\,pH - pK_1} + 10^{\,pH-pK_2}) + A_2/(1 + 10^{\,pK_1-pH} + 10^{\,pH-pK_2}) + A_3/(1 + 10^{\,pK_1-pH} + 10^{\,pK_2-pH}) \qquad (3)$$

A_1, A_2 and A_3 refer to the absorbance of LH_2H^*, LH^*H^- and LH^{2-} respectively in the presence of $Cu^{(II)}$. Fitting the experimental data according to equation (3) (Fig. 1Sd), the value for pK was 5.99 ± 0.20 and 8.97 ± 0.15 respectively. Using this value and equations 4-7 stability constant of the complex was determined in solution [2-4].

$$\beta^* = \frac{[Cu(LH_2)_2][H^+]^2}{[Cu^{2+}][LH_3]^2} \qquad (4)$$

$$Cu^{2+} + 2LH_2^- \rightleftharpoons Cu(LH_2)_2 \qquad (5)$$

$$\beta = \frac{\left[Cu(LH_2)_2\right]}{\left[Cu^{2+}\right]\left[LH_2^{-}\right]^2} \quad (6)$$

$$\beta = \frac{\beta^*}{K^2} \quad (7)$$

K refers to the equilibrium constant for the dissociation of phenolic-OH of LH_3 on C_1 [1]. The value for the formation constant (β) was determined from Eq. 7 and found to be 4.88×10^{15} comparable to reported stability constants of Cu(II) with doxorubicin [$(4.6 \pm 1.1) \times 10^{16}$] and sodium 1,4-dihydroxy-9,10-anthraquinone-2-sulphonate [9.64×10^{16}] [2,4].

The initial structural model for $Cu^{(II)}$-$(LH_2)_2$ that was used to arrive at the structure of the complex from PXRD data.

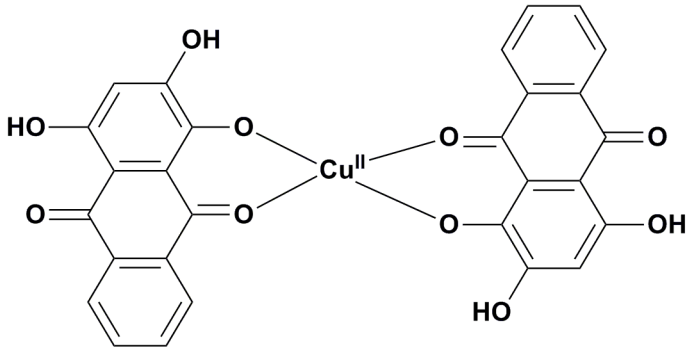

Expected/probable structure of Cu(II) complex of LH_3 or *trans*-[Cu(II)-$(LH_2)_2$]

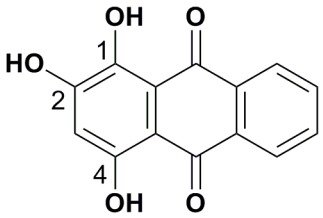

Ligand: 1,2,4-trihydroxy-9,10-anthraquinone or purpurin or LH_3

TDDFT of $Cu^{(II)}$-$(LH_2)_2$:

Table 1S. MO composition of $Cu^{(II)}$-$(LH_2)_2$ complex in triplet (S=1) ground state calculated by DFT/(U)B3LYP method in acetonitrile.

α-spin			
MO	**Energy (eV)**	**Composition (%)**	
		Cu	**LH_3**
LUMO+19	2.982	3	97
LUMO+18	2.673	77	23
LUMO+17	2.566	13	87
LUMO+16	2.285	5	95
LUMO+15	0.922	0	100
LUMO+14	0.876	1	99
LUMO+13	0.7	12	88
LUMO+12	0.659	13	87
LUMO+11	0.501	112	-12
LUMO+10	0.152	75	25
LUMO+9	0.103	84	16
LUMO+8	-0.178	106	-6
LUMO+7	-0.647	1	99
LUMO+6	-0.69	2	98
LUMO+5	-1.29	0	100
LUMO+4	-1.336	1	99
LUMO+3	-2.209	0	100
LUMO+2	-2.256	0	100
LUMO+1	-3.921	0	100
LUMO	-3.987	0	100
SOMO	-6.35	1	99
HOMO-1	-6.542	1	99
HOMO-2	-7.419	1	99
HOMO-3	-7.439	0	100
HOMO-4	-7.452	1	99
HOMO-5	-7.533	0	100
HOMO-6	-7.746	12	88
HOMO-7	-7.787	0	100
HOMO-8	-7.794	2	98
HOMO-9	-8.023	1	99
HOMO-10	-8.056	0	100
HOMO-11	-8.608	4	96
HOMO-12	-8.686	1	99

HOMO-13	-8.855	2	98
HOMO-14	-9.378	19	81
HOMO-15	-9.561	1	99
HOMO-16	-9.929	3	97
HOMO-17	-10.017	9	91
HOMO-18	-10.08	2	98
HOMO-19	-10.118	3	97
β-spin			
MO	**Energy (eV)**	**Composition**	
		Cu	**LH_3**
LUMO+19	2.663	72	28
LUMO+18	2.583	18	82
LUMO+17	2.306	5	95
LUMO+16	0.924	0	100
LUMO+15	0.877	1	99
LUMO+14	0.704	14	86
LUMO+13	0.663	13	87
LUMO+12	0.503	112	-12
LUMO+11	0.145	74	26
LUMO+10	0.11	84	16
LUMO+9	-0.112	104	-4
LUMO+8	-0.642	1	99
LUMO+7	-0.687	2	98
LUMO+6	-1.289	0	100
LUMO+5	-1.334	1	99
LUMO+4	-2.207	0	100
LUMO+3	-2.254	0	100
LUMO+2	-3.899	18	82
LUMO+1	-3.911	45	55
LUMO	-3.967	1	99
HOMO	-6.318	1	99
HOMO-1	-6.525	1	99
HOMO-2	-7.427	0	100
HOMO-3	-7.439	0	100
HOMO-4	-7.465	0	100
HOMO-5	-7.539	0	100
HOMO-6	-7.791	0	100
HOMO-7	-7.792	0	100
HOMO-8	-7.991	2	98
HOMO-9	-8.04	0	100
HOMO-10	-8.342	1	99
HOMO-11	-8.549	5	95
HOMO-12	-8.826	2	98
HOMO-13	-9.019	22	78

HOMO-14	-9.302	26	74
HOMO-15	-9.344	2	98
HOMO-16	-9.858	18	82
HOMO-17	-9.894	18	82
HOMO-18	-10.037	17	83
HOMO-19	-10.061	1	99

IR, EPR and Mass of $Cu^{(II)}$-$(LH_2)_2$

IR spectrum was recorded on a Perkin Elmer RX-1 spectrophotometer. Mass spectrum was recorded on Micromass Q-Tof micro™, Waters Corporation. Elemental analysis was carried out on a Perkin Elmer 2400 Series-II CHN analyzer. EPR spectrum was recorded in solid state in JEOL JES-FA 200 ESR spectrophotometer.

Analysis of the IR spectra

IR spectrum of LH_3 showed a peak at 3383 cm^{-1} characteristic of O–H stretching (Fig. S2) while the complex showed a broad band at 3436 cm^{-1} (Fig. S3). A complete absence of the peak at this region was however not observed for $Cu^{(II)}$-$(LH_2)_2$ since each LH_2^- bound to Cu(II) had two other -OH groups in the molecule. IR spectrum of LH_3 (Fig. S2) had a characteristic carbonyl stretching at 1670 cm^{-1} that was absent in $Cu^{(II)}$-$(LH_2)_2$ (Fig. S3) indicating the carbonyl oxygen was involved in binding the metal ion.

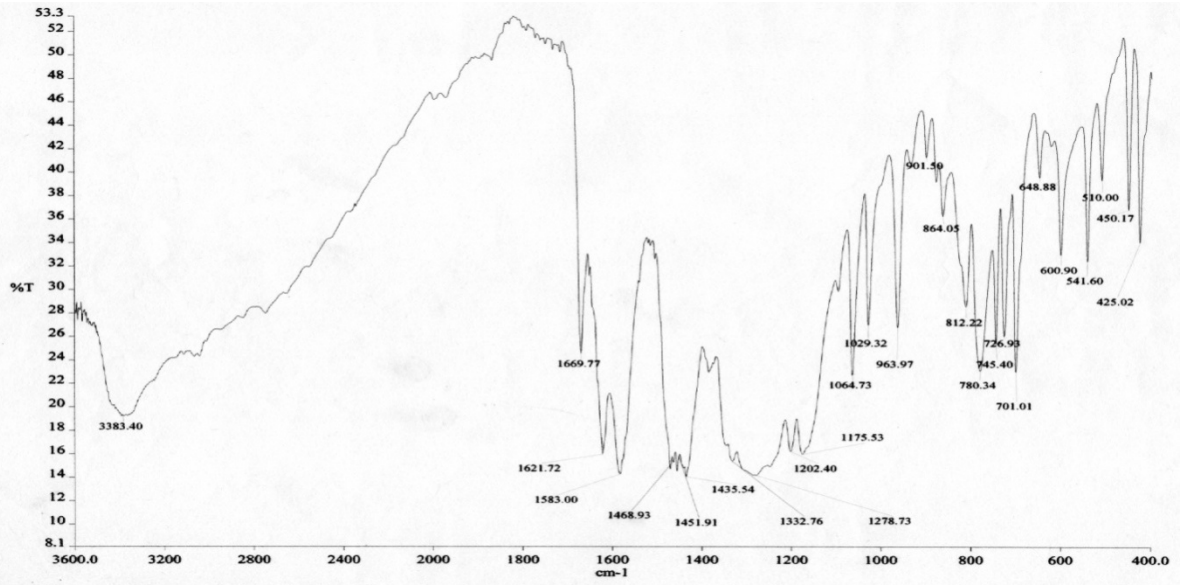

Figure S2. IR spectrum of LH_3.

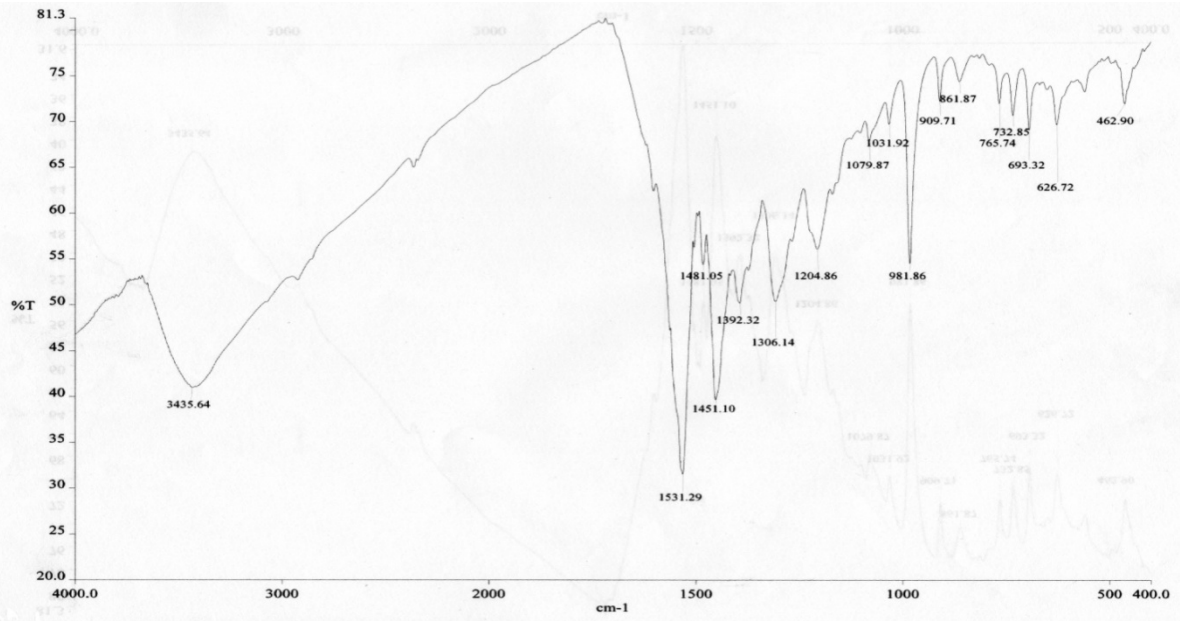

Figure S3. IR spectrum of $Cu^{(II)}$-$(LH_2)_2$ complex.

Analysis of Mass spectrum

The mass spectrum of $Cu^{(II)}$-$(LH_2)_2$ (Fig. S4) matched the crystal structure. The molecular ion peak was detected bound to sodium at m/z = 629.98 (^{63}Cu) and 632.0 (^{65}Cu) respectively. The most intense signals were at m/z = 354.27 (calculated m/z = 354.2) and 356.29 (calculated m/z = 356.2) respectively corresponding to a fragment that contained a Cu atom bound to one LH_3 and two molecules of water. The isotopic distribution for Cu tallied appreciably with the intensity of the two peaks (m/z 354.27 and 356.29). Dissociation of a molecule of water from this species (m/z = 354.2 or 356.2) along with loss of one or more hydrogens generated a peak having m/z = 337.2. Loss of the second water molecule resulted in the fragment (m/z = 311.2). A peak at m/z = 301.2 corresponds to a fragment where a Cu atom was bound to LH_3 from which a phenolic – OH departed.

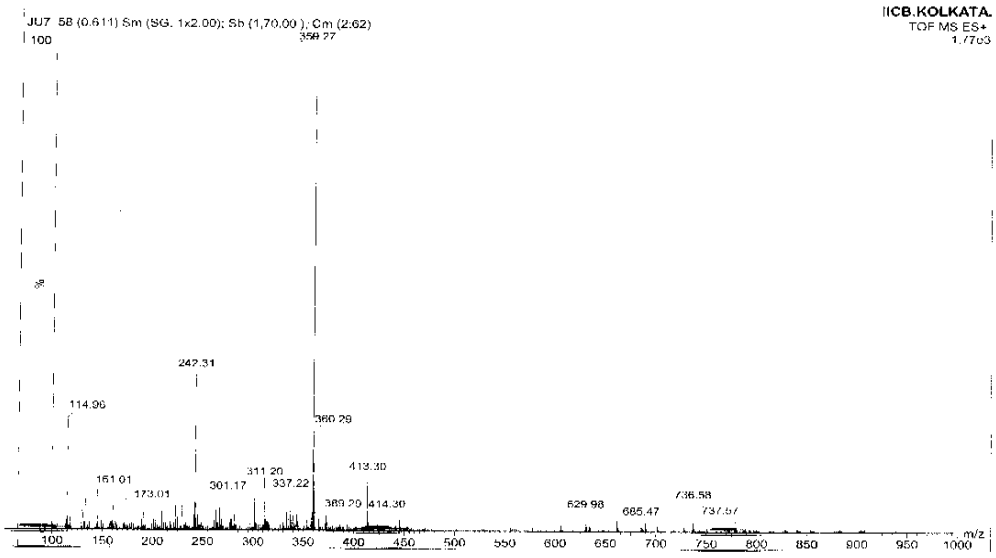

Figure S4. Mass spectrum of $Cu^{(II)}$-$(LH_2)_2$

EPR:

The EPR spectrum (Fig. S5) of $Cu^{(II)}$-$(LH_2)_2$ provides a *g*-value = 2.08 that was consistent with CuL_2 type copper complexes of 1-hydroxy-9,10-anthraquinone, 1,8-dihydroxy-9,10-anthraquinone [5] and of the anticancer drug adriamycin [6,7]. Spin density analysis by DFT study (Fig. 1h) revealed a mixed metal-ligand behavior of the paramagnetic complex as was experimentally found in the EPR spectrum. EPR spectral features of Cu^{2+} complexes of several hydroxy-9,10-anthraquinones were found to be similar to Cu^{2+}-ADM [5-7] that was assigned to species having tetragonal coordination structure indicating both systems form similar coordination complexes with Cu^{2+}. $Cu^{(II)}$-$(LH_2)_2$ shows signals in the field strength 250 to 350 mT attributed to CuL_2 type complexes mentioned above.

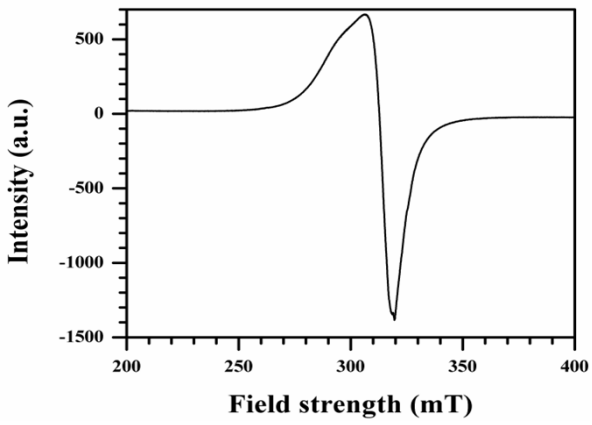

Figure S5. Low temperature (77 K) solid state ESR spectra of $Cu^{(II)}$-$(LH_2)_2$

CT DNA interaction of LH_3 and $Cu^{(II)}$-$(LH_2)_2$: UV-Vis study

Binding of the compounds with CT DNA was studied considering the following equilibrium on the interaction of small molecules with DNA.

$$L + DNA \rightleftharpoons L - DNA \qquad K_d = \frac{[L][DNA]}{[L - DNA]} \qquad (8)$$

Equation 8 considered in the reverse direction yields a double reciprocal Equation 9.

$$\frac{1}{\Delta A} = \frac{1}{\Delta A_{max}} + \frac{K_d}{\Delta A_{max}(C_D - C_L)} \qquad (9)$$

The decrease in absorbance (ΔA) on titrating each compound with CT DNA was used to create binding isotherms at different pH [8]. ΔA_{max} indicates the maximum change in absorbance following interaction of the compounds with CT DNA. C_D denotes concentration of CT DNA present in any aliquot and C_L the concentration of the compounds. K_d and ΔA_{max} was evaluated [1,9,10] utilizing equation 9.

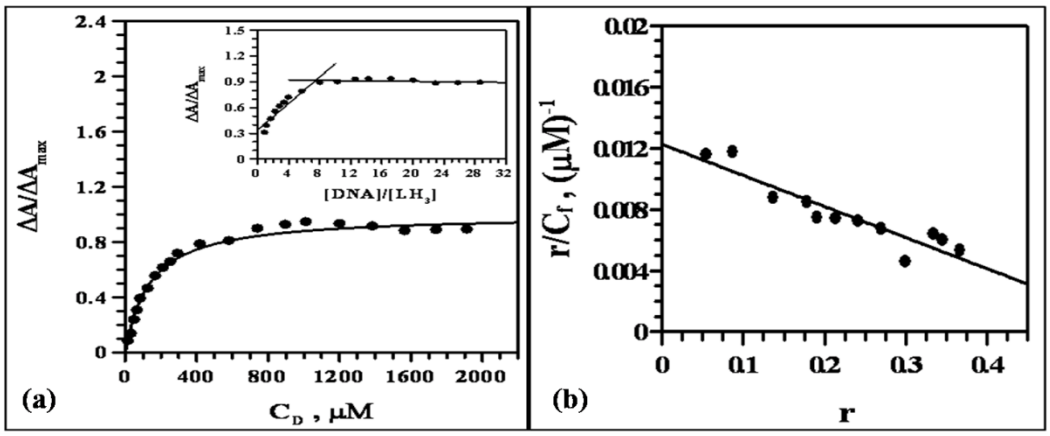

Figure S6. (a) Binding isotherm of the spectrophotometric study of LH_3–CT DNA interaction with the corresponding non-linear fit. Inset: Plot of normalized increase in absorbance as a function of the mole-ratio of LH_3 to CT DNA; (b) A Scatchard plot obtained for the interaction of LH_3 with CT DNA based on a titration followed by UV-Vis spectroscopy; [LH_3] = 75 μM, [NaCl] = 120 mM; [Tris buffer] = 15 mM at pH = 7.88; T = 298 K.

Change in absorbance was followed at the λ_{max} of LH_3 at the pH in which experiments were done. In the pH range 6.65 to 8.35, change in absorbance (ΔA) was followed at 513 nm. Fig. S6(a) being a typical plot of $\Delta A/\Delta A_{max}$ against concentration of DNA fitted by non-linear square fit analysis [1,9,10] (Eq. 10 & 11) to evaluate K_d at pH 7.8.

$$K_d = \frac{\left[C_L - \left(\frac{\Delta A}{\Delta A_{max}}\right)C_L\right]\left[C_D - \left(\frac{\Delta A}{\Delta A_{max}}\right)C_L\right]}{\left(\frac{\Delta A}{\Delta A_{max}}\right)C_L} \tag{10}$$

$$C_L\left(\frac{\Delta A}{\Delta A_{max}}\right)^2 - (C_L + C_D + K_d)\left(\frac{\Delta A}{\Delta A_{max}}\right) + C_D = 0 \tag{11}$$

The plot of $\Delta A/\Delta A_{max}$ against [DNA]/[LH_3] [Inset, Fig. S6(a)] at different pH was done to obtain "$n_{b,}$" the site size of interaction. Overall binding constant (K*) at each pH was obtained by multiplying K_{app} with "n_b".

The Scatchard equation (Eq. 12) [11] was also used to analyze the results obtained from UV-Vis titration of LH_3 with CT DNA. Overall binding constant (K*) and binding stoichiometry "n_b" was obtained directly [1,2] from Fig. S6(b).

$$r/C_f = K^*(n - r) \tag{12}$$

r = C_b/C_D where, "C_b" is the concentration of bound LH_3 and "C_D" the concentration of CT DNA. "C_f" refers to concentration of free compound. "K*" is the intrinsic binding constant or overall binding constant of any molecule binding to a substrate. "n" is the binding stoichiometry in terms of number of bound compound per nucleotide while "$n_{b,}$" reciprocal of "n" denotes

binding site size in terms of the number of nucleotide per molecule. K* values obtained from the Scatchard plot for LH_3 at different pH are summarized in Table 2S. It was observed as pH increased overall binding constant of LH_3 with CT DNA gradually decreased [8].

Table 2S. Results of the binding constants of LH_3 with CT DNA with the variation of pH at constant ionic strength of the medium.

pH	Intrinsic binding constant (M^{-1})
6.65	9.33×10^4
6.88	6.45×10^4
7.16	4.84×10^4
7.40	4.51×10^4
7.88	2.95×10^4
8.35	2.56×10^4

CT DNA interaction of $Cu^{(II)}$-$(LH_2)_2$: UV-Vis study

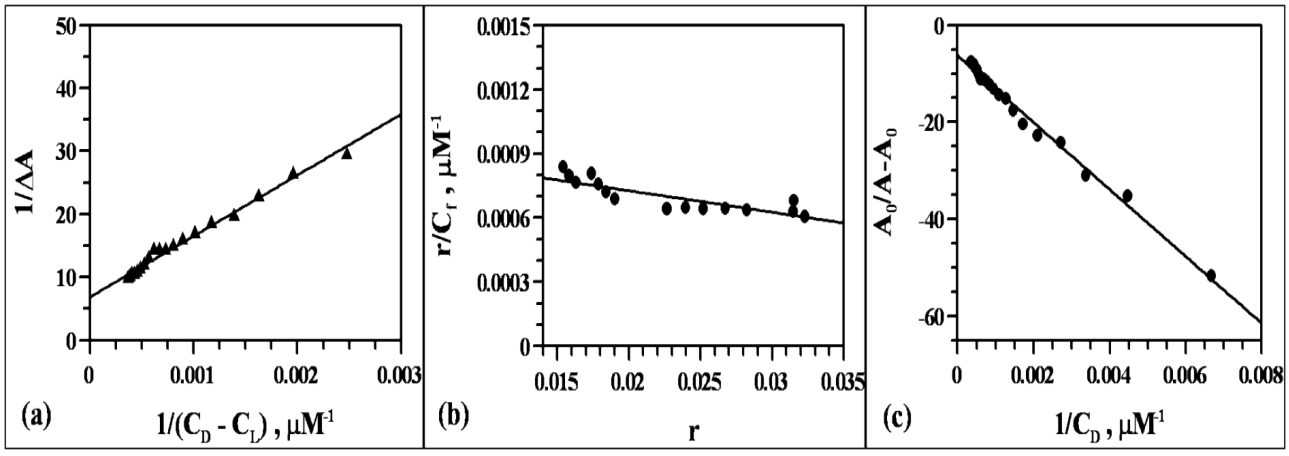

Figure S7. (a) Double-reciprocal plot of the interaction of $Cu^{(II)}$-$(LH_2)_2$ with CT DNA based on a titration followed by UV-Vis spectroscopy (b) Scatchard plot for the interaction of $Cu^{(II)}$-$(LH_2)_2$ with CT DNA; (c) Benesi-Hildebrand plot for the interaction of $Cu^{(II)}$-$(LH_2)_2$ with CT DNA; [$Cu^{(II)}$-$(LH_2)_2$] = 75 μM, [NaCl] = 120 mM; [Tris] = 15 mM of pH = 7.42; T = 298 K.

CT DNA interaction of $Cu^{(II)}$-$(LH_2)_2$: fluorescence study

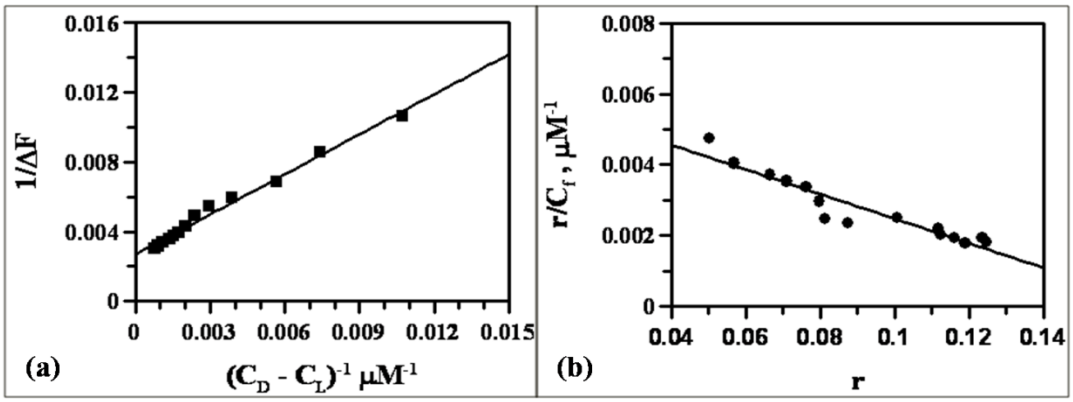

Figure S8. (a) Double-reciprocal plot for the interaction of $Cu^{(II)}$-$(LH_2)_2$ with CT DNA studied with the help of fluorescence spectroscopy. (b) Scatchard plot for the interaction of $Cu^{(II)}$-$(LH_2)_2$ with CT DNA; [$Cu^{(II)}$-$(LH_2)_2$] = 75 μM, [NaCl] = 120 mM; [Tris] = 15 mM of pH = 7.42; T = 298 K.

Kinetoplast DNA (kDNA) decatenation assay for topoismerase II enzyme

kDNA release assay for recombinant human topoisomerase II was performed in the presence or absence of the respective compounds by briefly incubating 100 ng of kDNA with 50 fmol of the enzyme in the reaction buffer supplied by the manufacturer (TopoGEN Inc.). DOX was used as the positive control drug that inhibits topoisomerase II by stabilizing covalent topoisomerase II-DNA complexes. DMSO concentration was maintained at 1% (vehicle control). Reactions were

incubated at 37°C for 30 minutes, loaded on 1% agarose gel with 0.5 µg/ml ethidium bromide and electrophoresis was done at 80 volts for 3 hours. On completion of electrophoresis, gels were viewed by Gel Doc 2000 (BioRad) under UV illumination. kDNA decatenation was assessed by monitoring the released kDNA minicircles in the gel.

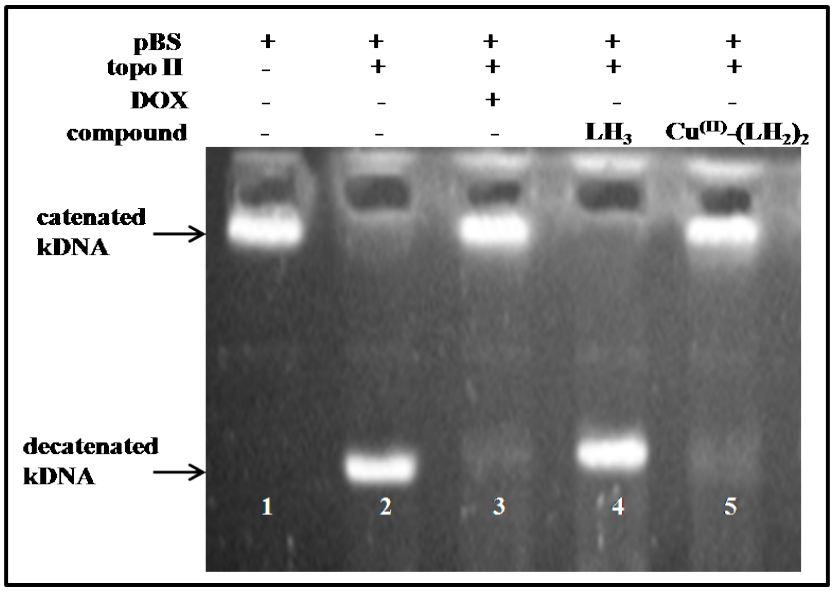

Figure S9. Kinetoplast DNA (kDNA) decatenation assay for topoismerase II enzyme. Lane 1:100 ng kDNA, lane 2:100 ng kDNA with 50 fmol topoisomerase II enzyme, lane 3: same as lane 2 but with 10 µM DOX, lane 4: same as lane 2 but with 20 µM LH_3, lane 5: same as lane 2 but with 20 µM $Cu^{(II)}$-$(LH_2)_2$. All reactions were incubated at 37 °C for 30 minutes and stopped with 0.5% SDS and analysed by agarose gel electrophoresis.

References:

[1] P. Das, P. S. Guin, P. C. Mandal, M. Paul, S. Paul**,** S. Das, J. Phy.Org. Chem. 24 (2011) 774.

[2] P. S. Guin, S. Das, P. C. Mandal, J. Inorg. Biochem. 103 (2009) 1702.

[3] S. Das, A. Saha, P. C. Mandal, Talanta 43 (1996) 95.

[4] H. Beraldo, A. G. Suillerot, L. Tosi, Inorg. Chem. 22 (1983) 4117.

[5] M. Tachibana, M. Iwaizumi, J. Inorg. Biochem. 30 (1987) 141.

[6] M. Tachibana, M. Iwaizumi, S. Tero-Kobuta, J. Inorg. Biochem. 30 (1987) 133.

[7] F. Morazzoni, A. Gervasini, Inorg. Chim. Acta. 136 (1987) 111.

[8] S. Mukherjee, P. Das, S. Das, J. Phy.Org. Chem. 25 (2012) 385.

[9] S. Roy, R. Banerjee, M. Sarkar, J. Inorg. Biochem. 100 (2006) 1320.

[10] S. Chakraborti, B. Bhattacharyya, D. Dasgupta, J. Phys. Chem. B 106 (2002) 6947.

[11] G. Scatchard, Ann. N. Y. Acad. Sci. 51 (1949) 660.